Development/Plasticity/Repair

Motor Axon Regeneration and Muscle Reinnervation in Young Adult and Aged Animals

Hyuno Kang and Jeff W. Lichtman
Department of Molecular and Cellular Biology and Center for Brain Science, Harvard University, Cambridge, Massachusetts 02138

Injuries to peripheral nerves can cause paralysis and sensory disturbances, but such functional impairments are often short lived because of efficient regeneration of damaged axons. The time required for functional recovery, however, increases with advancing age (Verdú et al., 2000; Kawabuchi et al., 2011). Incomplete or delayed recovery after peripheral nerve damage is a major health concern in the aging population because it can severely restrict a person's mobility and independence. A variety of possible causes have been suggested to explain why nervous systems in aged individuals recover more slowly from nerve damage. Potential causes include age-related declines in the regenerative potential of peripheral axons and decreases in the supply or responsivity to trophic and/or tropic factors. However, there have been few direct analyses of age-related axon regeneration. Our aim here was to observe axons directly in young and old mice as they regenerate and ultimately reoccupy denervated neuromuscular synaptic sites to learn what changes in this process are age related. We find that damaged nerves in aged animals clear debris more slowly than nerves in young animals and that the greater number of obstructions regenerating axons encounter in the endoneurial tubes of old animals give rise to slower regeneration. Surprisingly, however, axons from aged animals regenerate quickly when not confronted by debris and reoccupy neuromuscular junction sites efficiently. These results imply that facilitating clearance of axon debris might be a good target for the treatment of nerve injury in the aged.

Key words: **aging; axon regeneration; *in vivo* imaging; neuromuscular system; self-avoidance; synapse reinnervation**

Introduction

Unlike trauma to the CNS, injuries to peripheral nerves are often followed by complete recovery. The good outcomes are accounted for by the ease with which peripheral axons regenerate through endoneurial tubes to reoccupy neuromuscular junctions on denervated muscle fibers (Young, 1974; Rich and Lichtman, 1989; Nguyen et al., 2002). Nonetheless, regenerating axons must grow through a complicated milieu of cellular and molecular constituents during the reinnervation process. This environment mostly includes the contents of the endoneurial tubes that may be filled with glial cells, other axons, and debris from the former axons and/or their myelin ensheathment. Axons also must discriminate postsynaptic sites, nonsynaptic muscle fiber membranes, and the membranes of glial cell processes (Kang et al., 2007). Despite the complexity of the milieu, regenerating axons routinely reoccupy vacant synaptic sites and restore neuromuscular function. Because reinnervated neuromuscular junctions are nearly identical to their appearance before denervation (Rich and Lichtman, 1989), powerful mechanisms ensure reestablishment of the original pattern.

Received Sept. 20, 2013; revised Oct. 31, 2013; accepted Nov. 1, 2013.

Author contributions: H.K. and J.L. designed research; H.K. performed research; H.K. contributed unpublished reagents/analytic tools; H.K. and J.L. analyzed data; H.K. and J.L. wrote the paper.

We thank Drs. Miguel Vaz Afonso, Thomas Misgeld and Mike Sanderson for collaboration on building the 2 photon resonant galvanometer microscope.

The authors declare no competing financial interests.

Correspondence should be addressed to Jeff W. Lichtman, 52 Oxford St. Room 249.50, Cambridge, MA 02139. E-mail: jeff@mcb.harvard.edu.

DOI:10.1523/JNEUROSCI.4067-13.2013

 0270-6474/13/3319480-12$15.00/0

With advancing age, however, both the speed and magnitude of functional recovery is much reduced (Verdú et al., 2000; Kawabuchi et al., 2011). A number of ideas have been raised to explain slower recovery with aging, but the consensus is that axons regenerate slowly (Black and Lasek, 1979; Pestronk et al., 1980; Verdú et al., 1995). Several different factors to explain this slowdown have been suggested. Slowing might be related to an intrinsic change in the growth rate of old axons perhaps related to decreased axonal transport of cytoskeletal proteins (Brunetti et al., 1987; McQuarrie and Lasek, 1989; Tashiro and Komiya, 1994). Alternatively, old axons may have fewer trophic factor receptors and are less stimulated to grow (Uchida and Tomonaga, 1987; Ferguson and Son, 2011). Yet another idea is that the periaxonal milieu in old animals has less diffusible or bound extracellular factors (Komiyama and Suzuki, 1992; Martini, 1994; Bosse, 2012).

Evidence indicates that Wallerian degeneration is delayed in old animals (Tanaka and Webster, 1991; Vaughan, 1992; Kawabuchi et al., 1998). A potential consequence of slower Wallerian degeneration is delayed clearance of degenerating nerve debris. Myelin debris and axonal debris could have growth-inhibitory effects that curtail regeneration (McKerracher et al., 1994; Mukhopadhyay et al., 1994; Schäfer et al., 1996; Filbin, 2003). In addition, nerve debris per se may be a mechanical barrier. If this were the complete explanation, then axon growth rates in old animals would be normal except when axons face a mechanical barrier—exactly the result we found.

In the present work, we examine regenerating axons by time-lapse imaging to determine the rate of axon growth directly and immunohistochemistry. We show that axons in old animals do

grow at the same rates as axons in young animals, but that they are more frequently stopped by obstacles. We show that the obstacles are phagocytosed debris within Schwann cells. This result suggests that clearance of debris is a critical factor in the timely regeneration of peripheral nerves after damage.

Materials and Methods

Animals and surgery for denervation. Transgenic mice expressing cytosolic cyan fluorescent protein (CFP) or yellow fluorescent protein in motor neurons under control of the Thy1 promoter (Feng et al., 2000) were used for *in vivo* time-lapse imaging and immunohistochemistry. Brainbow animals (Membo-12) crossed with Thy1-Cre mice were used to label axons in multiple colors (Livet et al., 2007). To label Schwann cells, we crossed Thy1-CFP animals with S100-EGFP (enhanced green fluorescent protein) transgenic mice (Zuo et al., 2004). Two age groups, young adult (2–4 months) and aged adult (>20 months), of either sex were used.

For the denervation surgery, we anesthetized animals with a ketamine/xylazine mixture (0.10–0.15 ml of a 0.9% NaCl solution containing 17.4 mg/ml ketamine and 2.6 mg/ml xylazine). To denervate the triangularis sterni muscle, we crushed the intercostal nerve near the joint between the ventral and dorsal segments of ribs with #5 Dumont forceps. Regenerating axons in this muscle start to reoccupy vacant junctions ~5–6 d after nerve crush. To denervate the sternomastoid muscle, we crushed the muscle nerve just lateral to the muscle (lateral nerve crush) or ~6 mm proximal from the muscle (medial nerve crush). Regenerating axons in these animals start to reoccupy vacant junctions ~4 (lateral crush) and 6 d (medial crush) after the procedure. For the double nerve crush, we performed the second nerve crush 5 d after the first one, both at the medial crush site. Regenerating axons after double nerve crush start to reoccupy vacant junctions ~9–10 d after the first nerve crush. After each of these nerve crush procedures, the wound was closed with 6–0 suture and the animal was allowed to fully recover from the anesthesia in a warmed recovery chamber and then returned to its home cage.

Microscopy. Procedures for vital imaging in sternomastoid muscle were similar to those described previously (Rich and Lichtman, 1989; Zuo et al., 2004). *Ex vivo* imaging in triangularis sterni muscle were also performed as described previously (Kerschensteiner et al., 2008). Briefly, a mouse hemithorax was dissected out from a lethally anesthetized mouse and pinned down in a Sylgard (Dow-Corning)-coated 35 mm dish filled with oxygenated Neurobasal A medium (~35°C; Invitrogen) and then placed in the dish warmer (Harvard Apparatus). Throughout the experiment, we used oxygenated Neurobasal A medium by bubbling with 95% O_2/5% CO_2. After perfusing with Neurobasal A medium for 10 min, the triangularis sterni muscle was incubated with Alexa Fluor 594-conjugated α-bungarotoxin (BTX) for 5 min (1 μg/ml; Invitrogen) to label the postsynaptic acetylcholine receptors (AChRs). A thorough rinse with Neurobasal A medium was followed by continuous perfusion with the same solution (1 ml/min). The explants were then placed under a wide-field epifluorescence microscope (BX61; Olympus) for time-lapse imaging. Several different microscopes were used for *in vivo* time-lapse imaging: an Olympus FV1000, a Zeiss 510 with a Mai Tai multiphoton laser (Spectra Physics), and a custom made video-rate two-photon microscope (modified from Sanderson and Parker, 2003) equipped with a Mira 900 Ti-sapphire laser (Coherent) and 2 GaAsP PMTs (Hamamatsu). For two-photon microscopy, we used 800 nm light to simultaneously excite CFP and Alexa Fluor 594 fluorophores. An Olympus FV1000 confocal microscope was used to collect high-resolution image stacks from fixed samples.

Image processing and analysis. For the postimage processing and rendering, Photoshop (Adobe), MATLAB (MathWorks), MetaMorph (Molecular Devices), AutoQuant (MediaCybernetics), ITK-SNAP, and Fiji software packages were used. After we collected time-lapse movies, we removed out-of focus frames and then aligned the remainder either by automated software or, in some cases, manually. Because of jitter between frames, which is a consequence of imaging moving objects, and the limits of *xyz* optical resolution, we measured the extension length of the regenerating axon when it could reliably be measured to have grown 1–2 μm. These growth rates were measured at 5–15 min intervals depending on the quality of images and speed of axon regeneration. Overall growth rates were obtained by measuring the total extension length and dividing by the duration of the entire imaging session.

Immunohistochemistry. For some experiments, the muscle and attached nerve were removed, fixed in 4% paraformaldehyde in PBS, pH 7.4, for 1 h, and then rinsed in PBS. To label AChRs, either Alexa Fluor 594- or Alexa Fluor 647-BTX was used. Myelin was labeled with a polyclonal antibody against human myelin basic protein (A0623; Dako) with Alexa Fluor 594- or Cy3-conjugated goat anti-rabbit secondary antibody and Alexa Fluor 647-BTX.

Results

Regenerating motor axons in young adult mice face occasional obstructions as they traverse the nerve pathway back to muscle

To better understand the factors that adversely affect axon regeneration, we monitored regenerating motor axons that expressed fluorescent proteins in both young and old mice. Using time-lapse imaging, we followed regenerating motor axons as they grew back through endoneurial tubes and eventually reinnervated neuromuscular junction sites in explanted triangularis sterni muscle preparations (for details, see Materials and Methods and Kerschensteiner et al., 2008). The regeneration was induced 5–6 d before the explantation by a nerve crush ~5 mm proximal to the muscle's neuromuscular junction "endplate" zone. The explant usually remained healthy for several hours, during which time individual regenerating axons could be monitored many hundreds of times (Misgeld et al., 2007).

To get a sense of how normal young adult axons regenerate, we collected high temporal resolution (~1 image/10 s) time-lapse movies of 22 axons after nerve crush in 20 young adult mice (2–3 months of age). We discarded four of these time-lapse movies because these axons showed no signs of growth and may have been damaged or otherwise adversely affected by the explantation process. The remaining axons could be divided into two categories. First, 10 axons showed local dynamic changes in the shape of their tip or small organelle movements inside but also did not extend appreciably over the viewing session. Although these axons showed no growth during the imaging session, they were certainly able to grow because we were imaging many millimeters away from the site of nerve crush, meaning that these axons had already grown a long distance by the time we began monitoring them. We do not know why these axons did not regenerate while we were imaging and think it is more likely an artifact of our imaging methods than a biologically significant result. There were no obvious differences between the axons that did grow and those that did not in terms of axon caliber, axon shape, or fluorescence intensity. The other 8 axons grew during the imaging period (1–2 h). All but one of the growing axons failed to branch over the imaging session. The one axon that did branch generated a collateral side branch rather than bifurcating at its growing tip. The growing axons had on average an overall growth rate of ~0.9 μm per minute. However, there was substantial variation in rates (~7-fold) among the individual axons. The fastest axon advanced at ~1.5 μm/min and the slowest at ~0.2 μm/min. Regenerating speed appeared to be correlated with the axon's caliber: the fastest growing axon was the thickest and vice versa ($n = 7$, $r = 0.79$; Fig. 1*A*). Therefore, regenerating axons have intrinsically different growth rates that correlate with their calibers.

It was immediately obvious that, in addition to the variability in overall growth rates between axons, each axon also changed its growth rate over time. We found that the peak growth rates of individual axons did vary. However, for each axon, the peak growth rate (0.4–3.1 μm/min; Fig. 1*B*) was greater than the av-

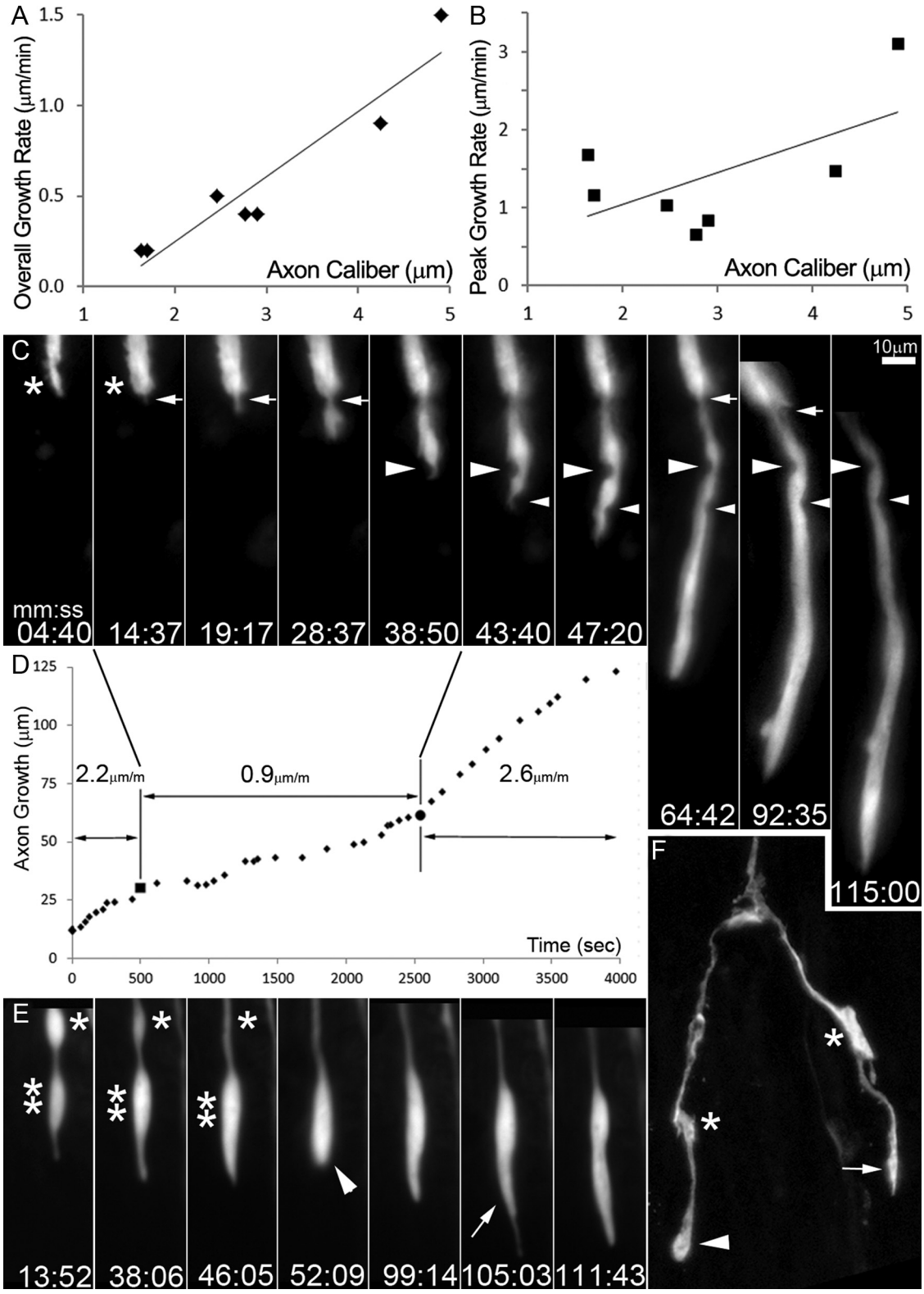

Figure 1. Regenerating axons in young animals slow when passing by obstacles. ***A***, ***B***, Graph showing that axon caliber correlates better to overall growth rate of regeneration (***A***) than peak growth rate (***B***). Caliber of individual regenerating axons (*x*-axis) and, on the *y*-axis, their overall regeneration rates and peak rates are plotted ($n = 7$). Correlation coefficient (R) is 0.79 for overall and 0.61 for peak rates. ***C***, A regenerating axon was monitored for 2 h in an explanted triangularis sterni muscle from a 3-month-old mouse 5 d after a crush injury. The axon decelerated, accelerated, and even paused while growing >100 μm. Deceleration and pause were associated with axonal indentations along the axon shaft (arrows and arrowheads). Because the indentations are maintained until the end of imaging session, we think the growth delays are associated with the axon attempting to pass by multiple space-occupying obstacles. After these delays, the axon grew rapidly and showed no additional indentations. See the Results for details. The overall growth rate was 1.5 μm/min and the axon caliber near the growth cone was $\sim$4.9 μm. ***D***, Graph showing a change in axon extension rate associated with obstacles in the path of the axon shown in ***C***. Two vertical lines mark what we believe are the beginning and the end of the obstacle zone, where the axon was indented and its growth rate slowed. ***E***, As axons regenerate, the axoplasm redistributes from a swelling into the distal compartment. An axonal varicosity (asterisk) just proximal to the growth cone (double asterisks) disappeared at the same time the growth cone added volume, suggesting that the axoplasm inside of the varicosity moved anterogradely (*Figure legend continues.*)

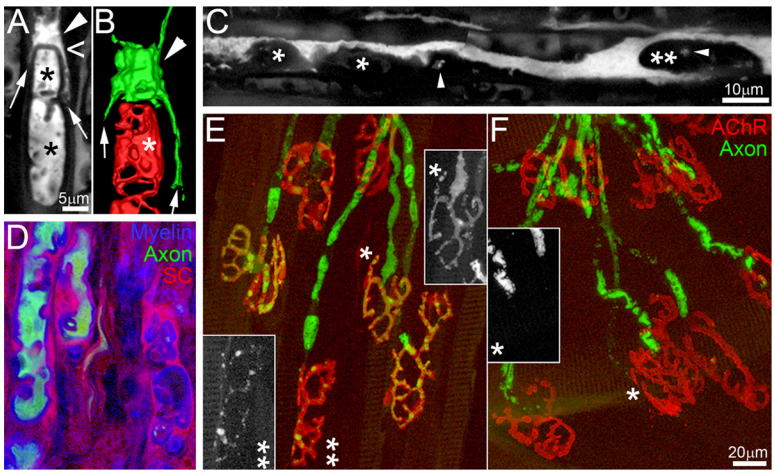

Figure 2. Degenerating axon and myelin debris impedes axon regeneration. ***A***, ***B***, Confocal imaging reveals the debris near the growth tip of a regenerating axon just distal to the site of nerve damage (nerve crush occurred 3 d previously). ***A*** is a confocal section and ***B*** is a 3D rendering of the entire confocal stack of the same axon. See Results for details. ***C***, Regenerating axons were also obstructed by nonfluorescent (i.e., non-neuronal) debris. Shown is a regenerating axon growing from the left of the figure, the shape of which was distorted by objects that are for the most part nonfluorescent (asterisks). As in the example shown in ***A*** and ***B***, this axon is sending small branches around a large obstruction (double asterisks). The small dots of fluorescence (arrowheads) in the dark objects may indicate that there is some axonal debris intermixed with non-neural debris. ***D***, Some of the nonfluorescent material in endoneurial tubes after nerve crush is glial. Transgenically labeled Schwann cells (red) and axonal debris (green) and immunolabeled myelin (blue) are all found densely packed in endoneurial tubes. ***E***, ***F***, Axonal debris disappears earlier at nerve terminal sites than in more proximal axonal pathways. Approximately 1 d after nerve damage, we noted axon fragmentation for the first time occurring asynchronously in different axons and terminals. For example, one junction in the same field of view still showed an unfragmented axon (asterisk in ***E***), whereas other axons and their junctions were in various stage of degeneration (double asterisk in ***E***). The debris was removed earlier from the nerve terminals than the more proximal nerve branches, as seen by the preservation of some fluorescent fragments in the axon when no fragments were visible at the junction sites (asterisk in ***F***). Insets in ***E*** and ***F*** show the axon-only view.

erage growth rate (0.2–1.5 μm/min; Fig. 1*A*), indicating that axons were not growing steadily. All of the axons (8/8) had growth rates that decelerated and accelerated in unpredictable ways and, in some (3/8), growth halted completely for several minutes at a time (Fig. 1*C*). The pauses were never longer than ~8 min. Comparison of Figure 1, *A* and *B*, shows that the average growth rate correlated better than the peak growth rate with the caliber of the axon. In fact, both small and large caliber axons could grow at similar rates, suggesting that the difference in the average growth rates may be related to slow downs or pauses rather than intrinsic axon growth speed. We found that the pauses were as frequent in axons with large caliber as in small axons, suggesting that the higher growth rates in large caliber axons are due to a briefer duration of the pauses or periods of slower rates (see Discussion).

In the axons that halted completely, we noted significant changes in the shape of the growth cone associated with the halts in forward growth. In each case, the distal tip broadened at the time the axon's forward growth stopped, giving the impression that axoplasmic material that was to be used for axon extension was now accumulating at the stalled distal end (Fig. 1*C*, asterisks). We noted similar pointed and blunt growth cones in acutely fixed regenerating peripheral motor nerves (Fig. 1*F*), suggesting that these shape changes (and hence the pauses) are not related to the imaging protocols we are using.

After the halts in axonal extension, in each case (3/3), a fine filopodial process protruded from the blunt tip and axon growth resumed. For example, in the series of images shown in Figure 1*C*, we monitored an axon for 2 h and it paused soon after the imaging started. When we began imaging, this axon was growing at a rate of 2.2 μm/min and then stopped abruptly. After pausing for ~7 min, the axon resumed its forward growth, but now with a much thinner process (Fig. 1*C*, arrows). The thin tip elongated for an additional 4–5 μm while becoming progressively thicker. As the axon continued its forward growth, it became thin at two additional sites (Fig. 1*C*, large and small arrowheads). Interestingly, all 3 sites where this axon thinned remained observable as sites of narrowing long after (>1 h) the growing tip had passed beyond those sites. The long-lasting indentations therefore are likely physical obstacles that the axon grew around to continue its path to its target muscle fibers. We present additional evidence in the next section. To detail the behavior of axons at these putative obstacles more precisely, we measured the rates of growth locally at the sites of slowing. We found that while the axons grew along the contours of these obstacle, their growth rate dropped to 0.9 μm/min—much slower than the velocity of the axon either before (2.2 μm/min) or after (2.6 μm/min) the obstacle zone (Fig. 1*D*). This result is representative of what we observed in all eight axons we monitored over time (Fig. 1*A*,*B*).

In addition to intermittent narrowing, in some cases, long stretches of the regenerating axon were quite thin in caliber with only occasional areas of swellings (Fig. 1*E*,*F*, asterisks). As already mentioned, axonal growth rates were correlated with axon caliber, meaning that these thin axons were growing more slowly than the larger axons. Our data do not provide a definitive explanation for why these axons are thin over such long distances. We hypothesize they are thin either because of a proximal obstruction such that only a small amount of axoplasm has been able to make it past that site or, alternatively, regenerating axons may be thin if the axon has branched numerous times such that only a small amount of axoplasm is available for any given branch. In either situation, when such a thin axon faces an obstruction, it slows even further and locally may swell just proximal to the obstruction site. Therefore, we see multiple varicosities in the thin axons and, when these varicosities form (due to an obstruction), the axon invariably slows and in some cases ceases forward movement for a time. We found that these varicosities sometimes persist, but in other cases they eventually disappear as axons resume growing (Fig. 1*E*, asterisk). These kinds of data show that the axon caliber is variable along the axon's length and can change at local sites over time.

Debris from degenerating axons and myelin perturb axonal regeneration

The data above raise the question of what is the nature of these obstructions. After nerve injury, the distal parts of damaged axons undergo Wallerian degeneration. If the nerve bundle is not

←

(*Figure legend continued.*) into the growing tip. Also note that when the tip is blunt (arrowhead), its forward progress is less than when it becomes more pointed (arrow). The growth rate of this axon was 0.2 μm/min and the axon caliber near the growth cone was ~1.6 μm. ***F***, The blunt tips are not an artifact of *in vivo* time lapse imaging because acutely fixed preparations the same structures were observed. Shown is a regenerating axon with two branches: one with a pointed tip (arrow) and the other with a blunt tip (arrowhead). Varicosities (asterisks) were also found in the same axon.

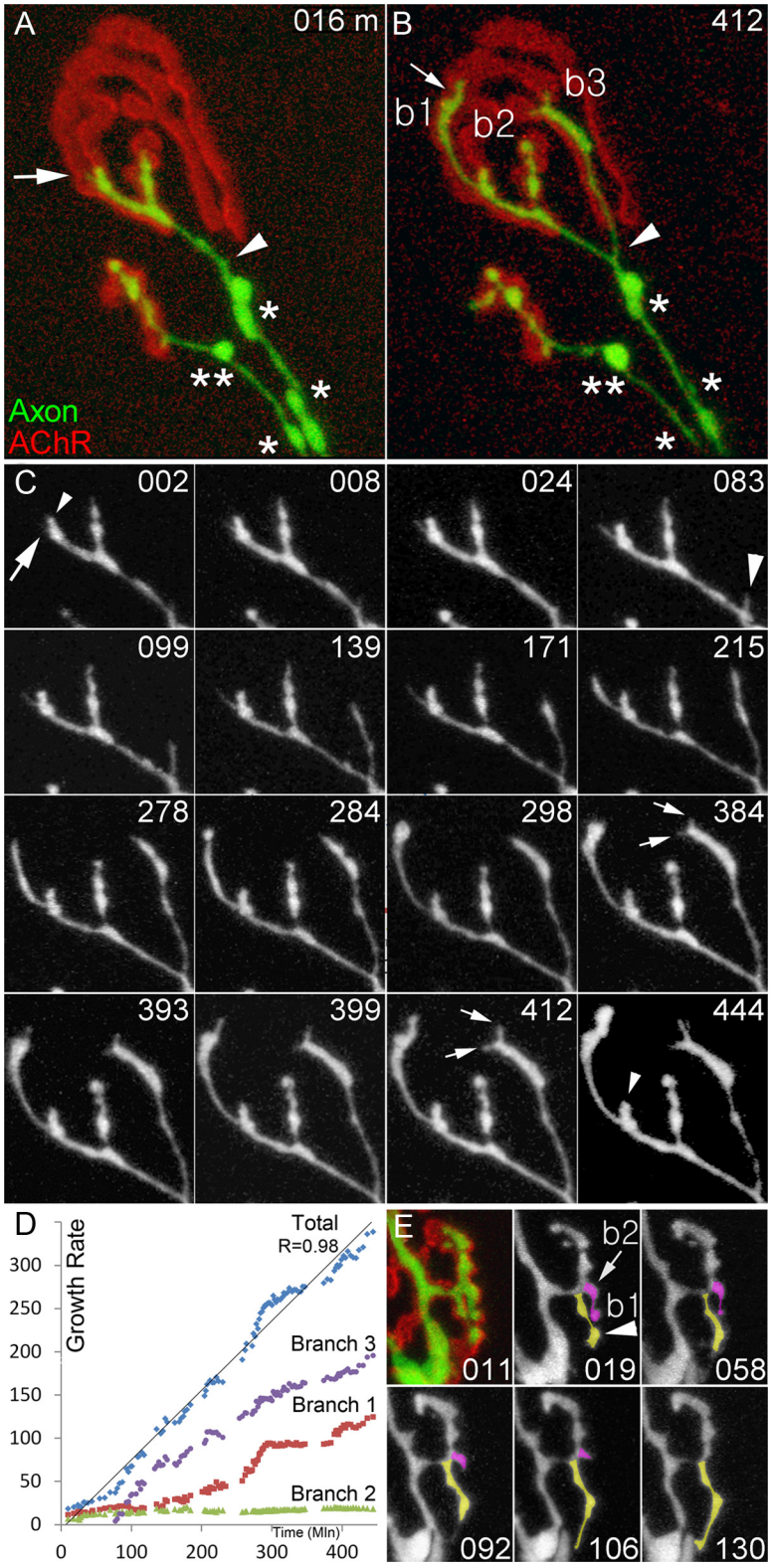

Figure 3. Regenerating axons reoccupy former neuromuscular junction sites in a piecemeal way. ***A–C***, A regenerating axon at a neuromuscular junction site 4 d after nerve crush (***A***) and 7 h later (***B***). This neuromuscular junction was imaged repeatedly *in vivo* for 7+ h in a 3-month-old animal. The reinnervating axon (green) added a collateral branch (***b3***) that originated from the axon shaft (arrowheads) just proximal to a large cluster of AChRs (red). Notice the shrinkage (asterisks) and swellings (double asterisks) in the caliber and size of varicosities of the axon. ***C***, Images taken every 3–5 min reveal the incremental pattern of synaptic regrowth. Although some branches were growing, others were quiescent. For example, branch b2 (***B***) grew very little over the 7 h, whereas branches 1 and 3 grew rapidly. The same phenomenon was seen at some sites where axon branches formed. Sometimes, one axon branch would grow and the other would not. For example, only one of the side branches of branch b1 grew extensively during this imaging session (large arrow vs small arrowhead). Conversely, branch b3 bifurcated and both of its daughter branches grew at similar rates, at least over the duration of this imaging session (small arrows). ***D***, Graph showing that the cumulative growth rates of regenerating branches of the same axon are not necessarily the same. Branch 2 (green, ***b2*** in ***B***) grew only slightly during the 7+ h imaging session. However, branch 3 (purple) grew linearly from the moment of its formation at 80 min of imaging and continuing until the end of the session 6 h later ($r = 0.96$). In contrast to the other two branches, axon branch 1 (red) changed rate a few times over the imaging session ($r = 0.93$). Despite the variability on the individual growth rates, the sum of their growth was strongly linear (blue; $r = 0.98$), suggesting that the branches of one axon at the same neuromuscular junction rarely paused at the same time. ***E***, One branch of a reinnervating axon (***b1***, tinted yellow) grew at the same time the other branch (***b2***, tinted purple) was retracting. It is possible that the cytoplasm that was in ***b2*** is used to generate the elongation of ***b1***.

physically transected (e.g., after nerve crush as opposed to nerve cut), the regenerating axons traverse paths that contain recently degenerated axons and thus may encounter debris originating from the previous axons, which could be an obstacle to regeneration. By the time regenerating axons arrive in the peripheral nerve at the sites we imaged, fluorescent fragments of the previously labeled axons were only rarely found. However, despite the general absence of fluorescent debris, it remains possible that there are nonfluorescent remnants from the former axons or their myelin sheaths. Immunostaining confirmed that myelin debris was present in endoneurial tubes every several micrometers 4 d after nerve damage (Fig. 6*E*). At this time point, we also saw a few small remnants of fluorescent axons. Over the subsequent few days, all signs of fluorescent debris disappeared, presumably as the fluorescent protein was digested by phagocytic cells. We also believe that the myelin debris continues to be digested over the subsequent several days because myelin immunostaining was weaker at 7 d than at 4 d after nerve crush. These results raise the possibility that the nonfluorescent obstacles in the way of regenerating axons are debris of the former axons and their myelin ensheathment.

To determine whether nerve debris is indeed the obstacle that impedes axon regeneration, we imaged regenerating axons as they first traversed the region beyond a nerve crush site (3 d after crush of the sternomastoid nerve). This early regrowth occurred at the time when fluorescent axonal debris was easily found throughout the nerve bundle distal to the crush site. We found many examples of situations in which generating axons were in close proximity to the debris of former axons (Fig. 2*A*,*B*, asterisks). The 3D deploy-

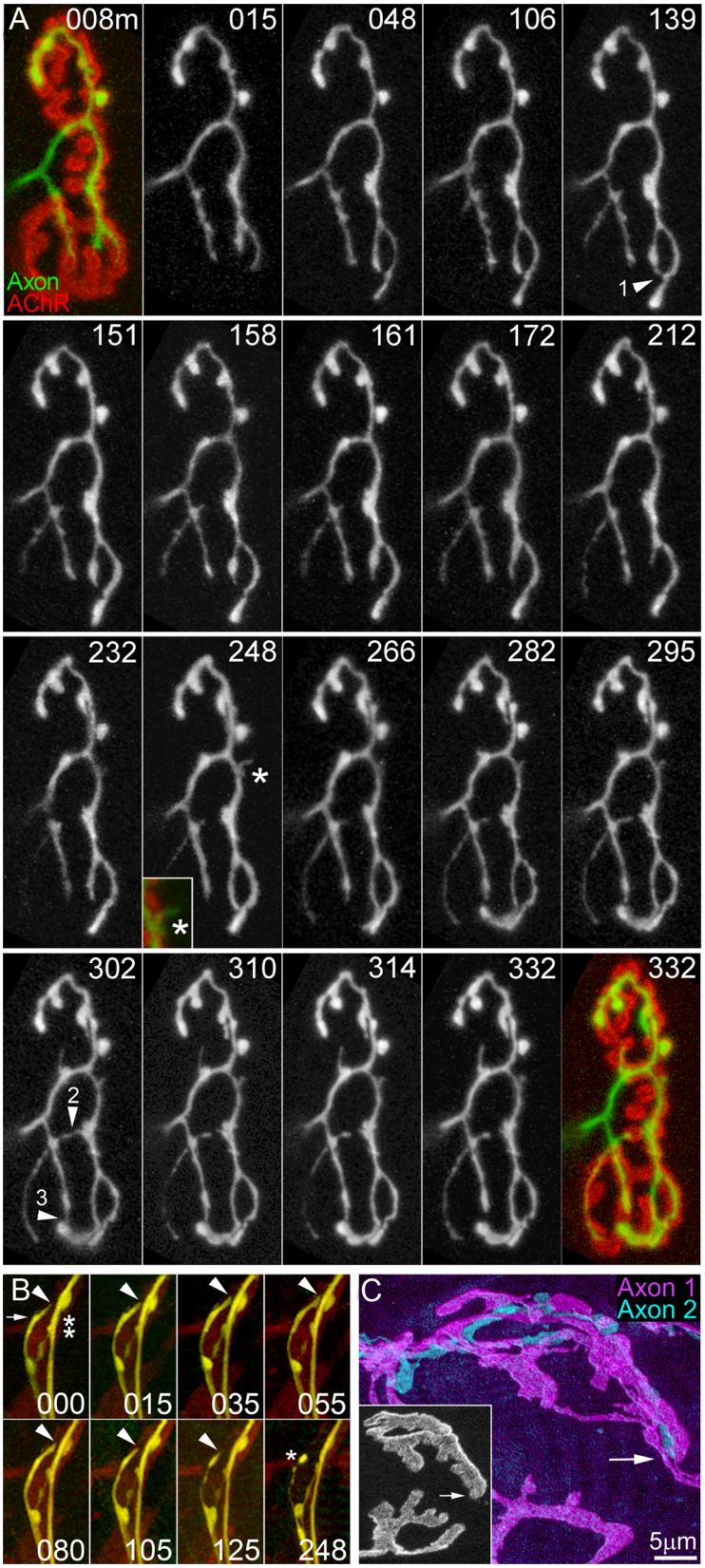

Figure 4. Regenerating axon branch tips retract to avoid persistent contact with other parts of the same axon. ***A***, Neuromuscular junction from a 3-month-old mouse 4 d after nerve crush imaged at the time an axon (green) is in the midst of reinnervating the former synaptic site (labeled red). In the time-lapse panels (18 images over 5 h), growth cones of regenerating axon branches can be seen to grow and then occasionally retract. Most of the retraction events occur within 10 min after the growing tip bumps into another part of the same axon (see arrowhead 1 at 139 min, arrowhead 2 and 3 at 302 min). ***B***, Growth cones of regenerating axons in nerve bundles also retract at sites where they transiently come into contact with other regions of the same axon. A growth cone (arrow) that originated as a terminal sprout at a neuromuscular junction was imaged repeatedly *in vivo* for 4+ h in the sternomastoid muscle in a 3-month-old animal 4 d after nerve crush. This sprout retracted after touching its parental axon shaft (double asterisks). Arrowheads indicate the end of the growth cone. ***C***, During nerve regeneration after double nerve crush (see Materials and Methods), different axons sometimes coinnervate the same primary synaptic folds. Shown is a region of a neuromuscular junction (inset) that is multiply innervated. The two axons (labeled purple and cyan) intermingle extensively without any signs of retraction. These results and others like it suggest that axon retraction is a phenomenon that occurs due to self-recognition.

ments of six axons were reconstructed from confocal stacks of the distal nerve. Unlike normal, nonregenerating axons or axons several weeks after regeneration, these showed a variable axon caliber with a scalloped appearance (Fig. 2*C*). Deeper scrutiny of the interface between axons and debris indicated that axonal growth was affected by the debris. In the example shown in Figure 2, *A* and *B*, a regenerating axon appears to confront a large aggregation of fluorescent protein labeled axonal debris (asterisks). Just proximal to the debris the axon shows a swelling (arrowhead) and bifurcates into two branches (arrows) that grow on either side of the debris mass. This tendency to bifurcate around sites of debris was commonly seen (Fig. 2*C*, double asterisks, shows axon branches circumventing debris). The debris was not always fluorescent (Fig. 2*C*), but even when the debris was fluorescent, the obstacle was typically larger than the fluorescent region because a dark edge could often be seen between the fluorescent debris and the regenerating axon (Fig. 2*A*). We think it likely that the nonfluorescent debris associated with degenerating nerves is usually degenerating myelin. Labeling with anti-myelin basic protein antibody reveals that axonal debris is often surrounded by myelin debris in endoneurial tubes (Fig. 2*D*).

Interestingly, it appears that synaptic debris is cleared more quickly than the remnants of more proximal axon branches (Fig. 2*E*,*F*). This difference may be due to the absence of myelin at the junctional sites and the greater exposure of axonal membrane at neuromuscular junctions to macrophages compared with multiple sheath layers that surround fasciculated nerves. Therefore, for nerve regeneration, the debris in the axon tracts is probably more problematic than at synaptic sites.

Regenerating axons reoccupy former synaptic sites with high fidelity

Once regenerating axons have negotiated their way back to neuromuscular junction sites, they must complete the essential regenerative step of reestablishing synapses with postsynaptic targets. We were interested to follow this final stage of regeneration at greater temporal resolution than has been done previously. We wanted to know the speed of neuromuscular reinnervation, whether axons paused at points during the reinnervation process as they did during the earlier steps, where and how axons branch to occupy all the AChR sites but end up with only a single branch in each primary synaptic fold, how they fill out their occupation of the former site (via lengthening vs thickening), and many other related issues associated with the reformation of synapses.

To answer these questions, we attempted to use the same *ex vivo* time-lapse imaging approach we used to study axon regeneration, but the reinnervation process required more time than our *ex vivo* preparations could be maintained. Therefore, to obtain longer observations, we monitored the reinnervation process of vacant neuromuscular junctions with confocal or 2-photon imaging *in vivo* within the sternomastoid muscle. We obtained 20 cases of axons reoccupying vacant junction sites over imaging sessions lasting 2–8 h (Figs. 3, 4). The results showed several things. First, once axons made contact with a former synaptic site, they appeared to continue to grow along former AChR rich sites with great accuracy (Fig. 3). Second, although axons occasionally sent small branches away from the junction, at these early reinnervation times, all of these branches (7/7) were resorbed over time intervals of several hours or less (Fig. 4). Third, in order for axons to reoccupy all of the former synaptic sites, they occasionally had to cross nonsynaptic regions to reach an island of AChRs. Our impression was that this crossing was not difficult for axons because they showed no appreciable delay at sites where they left AChR regions to grow briefly on non-AChR sites. This conclusion was reached using mice in which Schwann cells express GFP, which we crossed with transgenic mice expressing CFP in motor axons. Among the time-lapse movies of four junctional sites, we saw seven cases in which reinnervating axons crossed from one AChR rich cluster to another at sites where there was a preexisting glial bridge for the axon to grow along. Therefore, axons seem to be equally able to use former synaptic sites and glial bridges to reinnervate neuromuscular junctions efficiently.

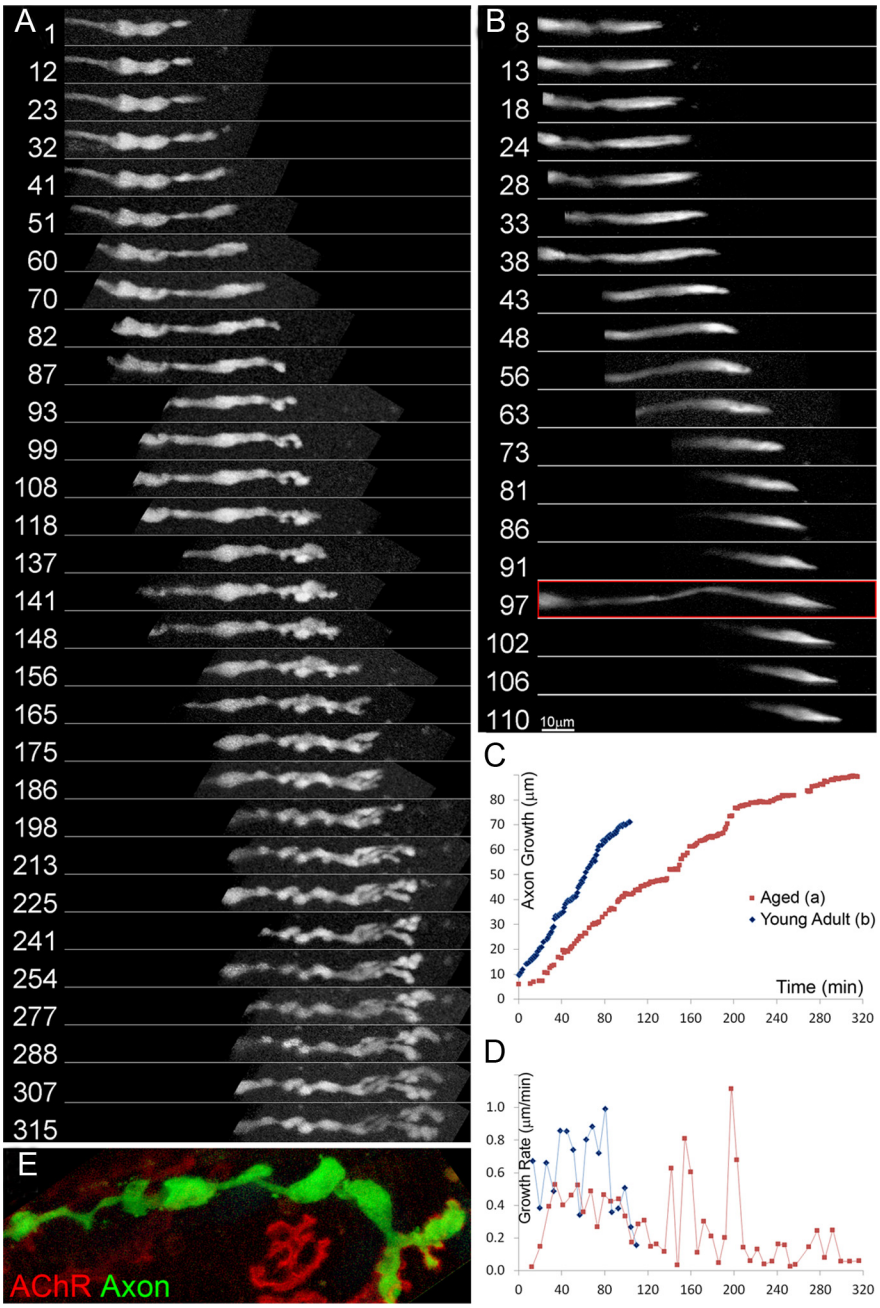

Figure 5. Regenerating axons grow haltingly and branch frequently in aged animals. ***A***, Shown is a 5 h *in vivo* time-lapse of axonal regeneration in a 23-month-old mouse 5 d after nerve crush. The growth cone forms several blunt tips and the axon caliber is not uniform. This appearance was seen in most regenerating axons in aged mice. ***B***, In contrast, regenerating axons in young mice such as in this 2-month-old were less branched and their tips were more pointed (red box). ***C***, ***D***, Cumulative growth curves (***C***) and changes in growth rates (***D***) show the slower overall growth for the aged axon shown in ***A*** (red) compared with the axon from a young animal shown in ***B*** (blue). Average growth rate was 0.6 μm/min in the young mouse versus 0.3 μm/min in the old animal. Both young and aged animals, however, accelerate and decelerate during the growth and had similar peak growth rates. ***E***, Acutely prepared samples from regenerating nerve-muscle preparations from aged animals (25 months old) show the same scalloped appearance as seen in preparations that were imaged over hours, indicating that this appearance is not an artifact induced by long-term exposure to light or other imaging-related artifacts. Axon is shown in green and postsynaptic AChRs in red.

The pace of reoccupation of synaptic sites by individual branches seemed to vary in speed and branches occasionally accelerated or decelerated during their forward progress. To investigate the behavior of individual branches of regenerating axons during reinnervation of neuromuscular junction site in detail, we measured growth rates of individual branches ($n = 17$) from four neuromuscular junctions. The growth rates were, on average,

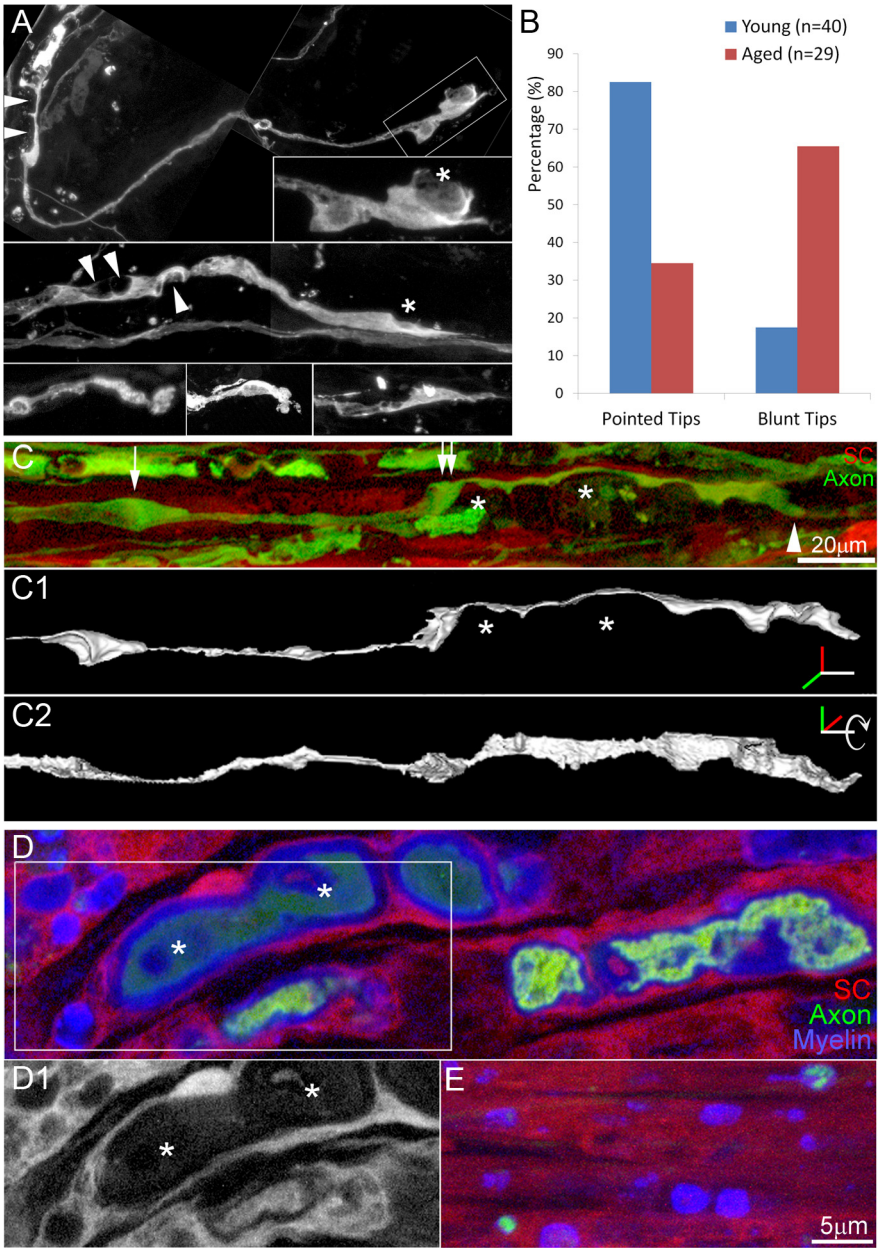

Figure 6. In aged animals, regenerating axons and their pathways were morphologically different from those in young animals. ***A***, Five examples of the distal tips of regenerating axons in 25-month-old mice. In contrast to young animals (Fig. 1), these axons were more irregular in caliber. At multiple sites along their length, they appeared to be indented by oval-shaped nonfluorescent masses (arrowheads). The tips of the growth cones were also more variable in shape compared with growth cones in young animals (Fig. 1). In some cases, the growth cone appeared to be squeezing by nonfluorescent objects in their way (asterisk). ***B***, There are significantly more growth cones with blunted tips in old animals compared with young animals ($p < 0.001$). ***C***, Evidence that axons squeeze between the edge of the endoneurial tube and vacuolated Schwann cells. Shown is a regenerating axon (green) in a regenerating nerve bundle from a 29-month-old mouse. Vacuoles (asterisks, see also ***D1***) in Schwann cells (red) appeared to push against the axon. Confocal reconstructions of this axon from two different rotation angles (***C1***–***C2***) revealed that it was actually a flattened ribbon. At the middle of the trajectory (double arrows), the axon can be seen to move from the bottom of the tube to the top, presumably because of an obstruction (asterisks) in its path. ***D***, Vacuoles in Schwann cells after nerve damage contain myelin debris. Immunolabeling myelin basic protein showed that the vacuoles in Schwann cells (red) contained myelin debris (blue) and axonal debris (green) from a 24-month-old mouse 4 d after denervation. A Schwann-cell-only image of the boxed area (***D1***) show dark Schwann cell vacuoles where axonal and myelin debris are located. ***E***, Far less debris was seen in 3-month-old animals 4 d after nerve damage (labeled the same way as in ***D***).

0.09 μm/min (±0.08 SD) and ranged from −0.04 to 0.23 μm/min. This rate is approximately an order of magnitude slower than axon regeneration in the nerve bundle (~0.9 μm/min; Fig. 1*A*). However, when the total extension of all of the branches to a neuromuscular junction was summed, the average cumulative growth rate was somewhat faster at 0.28 ± 0.08 μm/min ($n = 4$). For individual branches (even of the same neuron to the same neuromuscular junction), the speed did vary between them and for each one the speed varied over time. Some branches ($n = 2$) even retracted during the imaging session. This variation may not be random because in the few cases where it was possible to simultaneously measure several branches in the same neuromuscular junction, we found that the elongation of different branches was linked such that the cumulative elongation of the cohort of branches remained relatively constant (Fig. 3*D*). In some cases, branches were retracting while others were growing. For example, in Figure 3*E*, branch 1 (tinted yellow) can be seen to be growing at the same time that branch 2 (tinted purple) is retracting. We think this result is analogous to what we described above for axon regeneration before reaching the neuromuscular junction, where there were many instances of redistribution of axoplasmic material from a varicosity to the growing axon tip (Fig. 1*E*). Such shrinking (and expansion) of varicosities were also observed during the reinnervation of neuromuscular junctions (Fig. 3*A*,*B*, single and double asterisks). These rapid caliber changes in swelling or lengths show that the axonal cytoskeleton and membrane are elastic. Moreover, the flow of axoplasmic material out of a varicosity or side branch might be due to pressure differences between varicosities and growth regions that suck material from swollen regions to growth areas in much the way a child's balloon animal can redistribute the swellings by pulling on a region to create a pressure gradient.

Axon growth cones avoid sustained contact with other regions of the same axon

Despite the fact that an axon produces a number of branches to reoccupy all of the receptor rich areas, only one branch occupies each primary fold (as is the case in normal neuromuscular junctions). We used *in vivo* time-lapse imaging to understand why multiple branches never cooccupy the same primary junctional fold. We found that whenever a growth cone happened to touch another side branch or growth cone of the same axon, it underwent retraction (Fig. 4*A*). We documented 14 cases of this kind of retraction in the 20 time-lapse movies of neuromuscular reinnervation and found no clear examples of the cofasciculation of two branches of the same axon. We observed a similar avoidance phenomenon in the nerve bun-

dles where occasional axon sprouts contacted their parent axons and this also led to sprout retraction (Fig. 4*B*).

We were interested in determining whether the avoidance of prolonged contact occurred both between axon branches of the same axon and axon branches of different axons. We induced multiple innervation of neuromuscular junctions by double crush (for details, see Materials and Methods and Rich and Lichtman, 1989) using Brainbow animals so that we could visualize individual axons as being from different parent neurons by their different colors (Livet et al., 2007). We found several cases where two different reinnervating axons occupied the same primary synaptic fold (Fig. 4*C*), indicating that axons only avoid other branches of the same parent. This intermingling during reinnervation is similar to what is seen in normal developing neuromuscular junctions (Tapia et al., 2012).

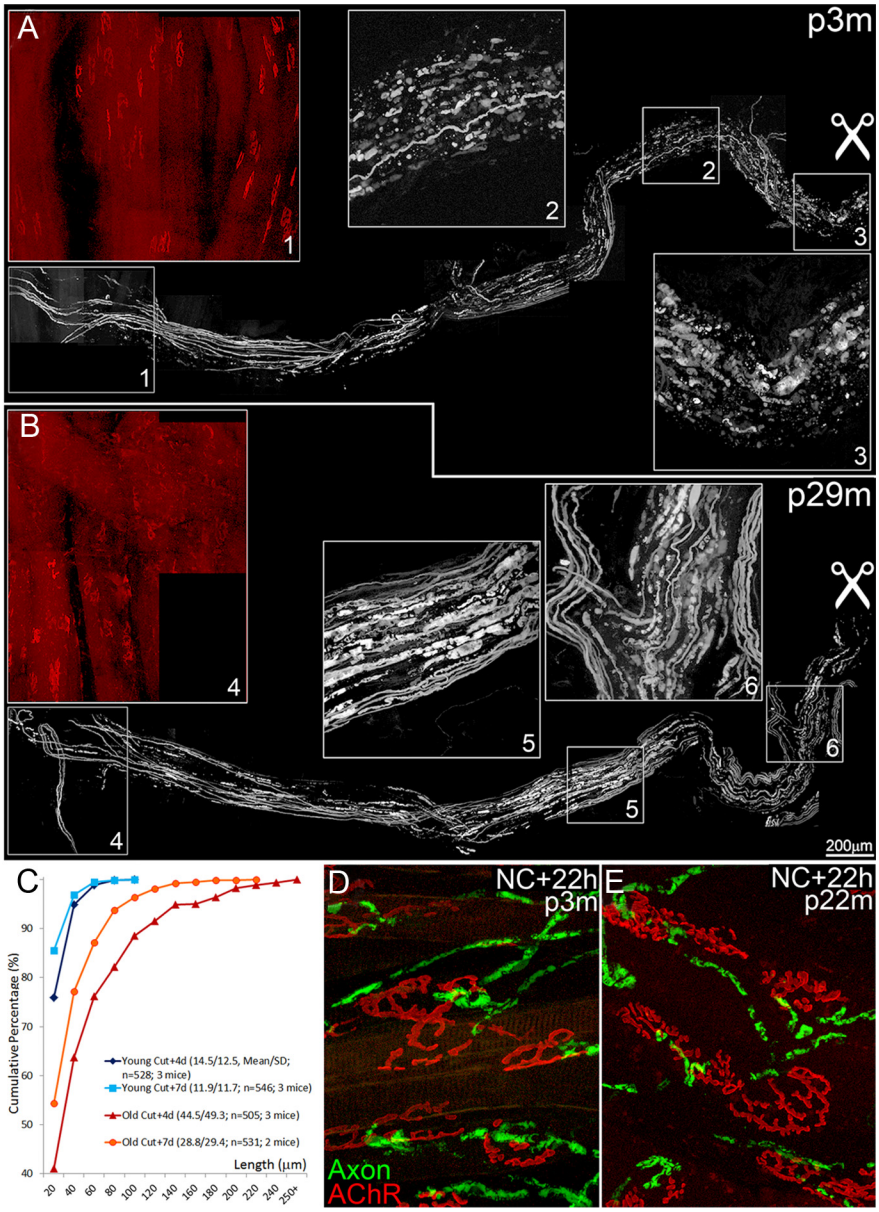

Figure 7. Debris clearance after nerve damage is retarded in aged animals. ***A***, ***B***, Evidence of a greater abundance of debris 4 d after nerve damage in old versus young animals. Reconstructions of the distal axon bundles from sites of nerve cut (scissors symbols) to sternomastoid muscle neuromuscular junction sites (red in box 1 and 4) in young adult (3 months old; ***A***) and aged (29 months old; ***B***) animals. Shown is fluorescently labeled axonal debris from a transgenic mouse that expresses CFP in its axons. AChRs were labeled with Alexa Fluor 594-conjugated BTX. Insets show evidence of the more numerous and larger debris fragments in the aged compared with the young adult animal. ***C***, Cumulative graph showing larger axonal fragmentations in aged animals (29 months old) than in young animals (3 months old; $p < 0.0001$). The increase was evident both 4 and 7 d after nerve cut (see Results for details). ***D***, ***E***, Evidence showing that initiation of debris formation occurred at a similar rate in young and old animals. Neuromuscular junctional areas (AChRs are shown in red and axons in green) were imaged 22 h after denervation in young adult (***D***) and aged (***E***) animals. The similarity of the degenerating axons in these two situations suggests that the onset of Wallerian degeneration was not delayed in old animals.

Regenerating axons in aged animals differ from those in young animals

Axon regeneration and reinnervation in aged animals is slower than in young animals (for review, see Verdú et al., 2000; Kawabuchi et al., 2011). To investigate the underlying causes, we imaged the sternomastoid muscle of 2 year-old mice 5–6 d after nerve crush at the time motor axons were first returning to the neuromuscular junction sites. A 2-year-old mouse is probably equivalent to a human in the mid- to late 60s assuming the maximum human lifespan is ~100 years (3 years for this breed of mouse). In the young animals with a nerve crush at the same site, the time to reach the neuromuscular sites was only ~4 d after nerve crush. To understand why the process took more time in aged adults, we tabulated the speed of axon regrowth over several hours in both young and old animals (Fig. 5*A*,*B*). Interestingly, in many respect, axons behaved similarly in young and old animals. For example, peak velocity was 1.0 and 1.1 μm/min in young and aged animals, respectively (Fig. 5*D*). Average rates over the entire imaging session, however, were slower with advanced age (0.6 vs 0.3 μm/min in young and aged animals, respectively; Fig. 5*C*). Moreover, as in young animals, axons in aged mice showed many decelerations and accelerations and occasional complete stops (Fig. 5*D*). Also as with young animals, the regenerating axons appeared to be growing within endoneurial tubes coursing in straight lines over many tens of micrometers.

There were, however, several differences in axonal behavior between young and old mice. Unlike the overall smooth contours of growing axons in young mice, the axons in aged mice had rough-appearing surfaces and possessed more varicosities (Fig. 5*A*,*B*). These varicosities were seen in acutely prepared samples as well as the time-lapse samples (Fig. 5*E*) and so are not an artifact induced by imaging old animals. The growth cones also were different in that they possessed significantly ($p < 0.001$, χ^2 test; Fig. 6*A*,*B*) more blunt tips than in young mice and there was more frequent growth tip branching. This difference in growth cone shape was quantified by analyzing high-resolution confocal stacks of growth cones in young ($n = 40$ in 5 animals) and old ($n = 29$ in 3 animals, 25 months old) mice during regeneration in

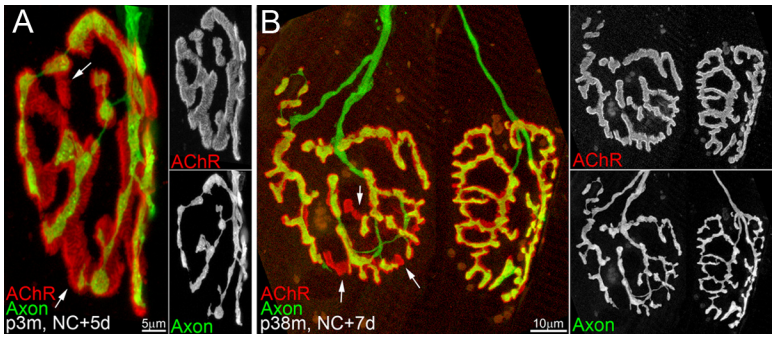

Figure 8. Regenerating axons reoccupy junctions in old animals as well as axons do in young animals. ***A***, Axons in the midst of reoccupying former synaptic sites in young animals quickly cover most of the AChRs. The few unoccupied sites (arrows) will likely be reinnervated within the next few days. ***B***, Axons also appear to successfully reoccupy receptor sites in old animals, because there are only a few unoccupied sites 1 week after nerve crush.

the sternomastoid muscle. In young mice, the tips of most (82.5%) of the reconstructed axons were narrower than the caliber of the proximal axon (i.e., "pointed" tips; Fig. 1*C*,*D*, arrows), whereas a minority (17.5%) had fatter or "blunt" tips (Fig. 1*C*,*D*, asterisks). In aged animals, the percentages were approximately reversed: fewer (34.5%) were pointed and more (65.5%) were blunt (Fig. 6*B*). We take this reversal to mean that there is a greater incidence of obstructions in the path of regenerating axons in old compared with young animals.

Slower clearance of axonal and myelin debris impedes regeneration in aged animals

To discover the source of the obstructions in the endoneurial tube, we studied regeneration in aged mice in which Schwann cells expressed fluorescent protein transgenically. We reconstructed the distal 200+ μm of a regenerating axon 4 d after nerve crush in a 29-month-old animal and found that the scalloped appearance was due to nonfluorescent vacuoles located within Schwann cells (Fig. 6*C*, red; Fig. 6*D1*). In the example shown, these vacuoles appeared to cause an obstruction that flattened the axon into a ribbon (Fig. 6*C1*,*C2*, asterisks). These images suggest that debris from the former axonal occupants of these tubes is responsible for the obstructions that alter the shape of regenerating axons. This conclusion was strengthened by immunostaining for myelin basic protein, which showed that these vacuoles (Fig. 6*D1*) contained myelin (Fig. 6*D*, blue).

These results suggest that debris is cleared more slowly in old animals than in young ones. To test this idea, we quantified fluorescent debris disappearance after nerve cut in young and old animals (Fig. 7*A*,*B*). In young animals, fluorescent fragments occupied ~13.6 ± 7.8% ($n = 75$) of the box (50 × 50 μm^2) located within the nerve bundle 4 d after denervation. In contrast, the density of degenerating axon fragments in aged animals was 23.2 ± 8.8% ($n = 75$; $p < 0.0001$, *t* test). When we examined the amount of debris remaining 3 d later (7 d after nerve cut), we saw a significantly greater decline in fluorescence in the young versus the old animals. In particular, of the fluorescent debris present at 4 d, there was a 25% drop at 7 d in the young mice ($n = 74$), whereas there a significantly smaller 17% drop in fluorescence in old mice ($n = 51$; $p < 0.0001$).

The loss of fluorescence was due to the gradual breakdown of large fluorescent compartments into smaller ones. For example, at ~1 d after nerve damage, the fluorescent fragments are quite large in young animals (Fig. 2*E*). By 4 d after nerve cut, however, the debris fragments were much smaller in average size. Therefore, the average length of the fragments declined over time. This decline in size continued into subsequent days. For example, in young animals, fragments were on average 14.5 ± 12.5 μm at 4 d after denervation, but only 11.9 ± 11.7 μm in 7 d after denervation ($p < 0.0001$, *t* test; Fig. 7*C*). The lag in debris clearance was also evidence by looking at the size of fragments in aged animals, in which the length of fluorescent fragments was substantially longer at 4 d after nerve cut (44.5 ± 49.3 μm, $p < 0.0001$). The debris continued to be degraded more slowly in old animals: the fluorescent debris was still 28.8 ± 29.4 μm at 7 d after nerve damage, significantly larger than the size and size distribution of the debris at the same point after nerve damage in young animals ($p < 0.0001$; Fig. 7*C*). These results suggest that Wallerian degeneration occurs more slowly in aged animals and as a result leaves more axonal and myelin debris in the endoneurial tubes, which, based on their ability to obstruct the endoneurial pathway, hinders axon regeneration. Importantly, our result also shows that the slowdown in debris clearance is not related to a more protracted start to debris formation: we compared the initiation phase of degeneration and found little difference between young and aged animals (Fig. 7*D*,*E*).

Regenerating axons accurately reoccupy junctional sites in old animals with no obvious differences from the reinnervation process in young animals

As already described, functional recovery after nerve injury is delayed in aged animals. Part of the problem we have shown is with the rate of axonal regeneration. We were also interested in determining whether the reinnervation of neuromuscular junctions per se is also negatively affected by age. Previous work (Valdez et al., 2010) showed that neuromuscular junctions in aged animals typically appear to be less well occupied by axons than junctions in young animals, suggesting that advanced age causes a defect in axonal recognition of, or adhesion to, postsynaptic sites. We were thus interested to learn to what degree the processes of nerve growth over former synaptic sites and reformation of the neuromuscular junction was adversely affected by aging.

We collected images of neuromuscular junctions from aged animals 7 d after nerve crush. Given the slower nerve growth in old animals, the 7 d interval between crush and imaging is equivalent to the reinnervation progress at 5 d after nerve crush in young adult mice. In 2- to 3-month-old mice, we found that at 5 d after nerve crush, axons had reoccupied 76 ± 24% of the neuromuscular junction AChR area ($n = 40$ junctions from 6 animals). We found a similar result in old animals, in which we imaged 42 junctions from 5 38-month-old animals 7 d after nerve crush injury. In the old animals, the reinnervating axons occupied 79 ± 21%: not significantly different from the reoccupation vigor of younger axons (Fig. 8). Regenerating axons in all but one junction showed good overlay on AChRs. The one exceptional junction showed a number of abnormalities including both faint and fuzzy receptor staining, suggesting that the muscle fiber itself was abnormal. These results suggest that, surprisingly, aged axons navigate to and reoccupy former neuromuscular junction sites, as is also the case in younger animals.

Discussion

Paralysis and muscle weakness are serious threats to the survival of an animal in the wild. Therefore, when motor nerves are damaged, rapid and efficient restoration of muscle function must be a high priority for the nervous system. The principle aims of this study were to explore the strategies used to reestablish neuromuscular connectivity after nerve injuries and to determine whether any of these strategies are adversely affected by aging. Using a combination of high-temporal-resolution *in vivo* recordings of regenerating nerves, high-resolution confocal microscopy, and immunostaining, we tracked axonal regeneration in young adult and aged animals. Several results were unexpected. First, we found that axons need to circumvent nerve degeneration debris in their paths to successfully reinnervate muscle fibers. Second, axons that were large caliber regenerated more quickly than smaller caliber axons despite having no substantial difference in peak growth rates. The reason for this difference is not known, but, given the debris obstacles that need to be overcome, this result suggests that larger axons can push their way through an obstacle easier than smaller axons. This idea of pressure exerted by an axon was also consistent with the way axons reoccupied neuromuscular junctions (Fig. 3). Third, upon returning to vacated neuromuscular junction sites, regenerating axons quickly reoccupy former synaptic sites without sending multiple branches along the same site by a mechanism of self-avoidance. Fourth, as others have described, the total pace of regeneration in aged animals was significantly slower. However, we discovered that the cause of this slowdown is explained by the reduced rate of clearance of axonal and myelin debris in peripheral nerves in old animals and, consequently, more physical obstacles in the paths of regenerating axons. Surprisingly, both unimpeded peak axon growth rate in the peripheral nerve and the reinnervation growth required to reoccupy neuromuscular junctions occurred similarly in young and old animals.

Our results partly corroborate and partly contest conclusions reached previously by electron microscopic sampling of regenerating nerves in young and old animals (Vaughan, 1992). In this previous study, the pace of axonal debris clearance after nerve damage was slower in old animals than in young animals and we found this to be the case as well. The electron microscopy study, however, did not reveal obstructions in the nerve, so the investigator ruled out the possibility that regenerating axons were impeded by objects in their path that blocked their way. In contrast, we found sporadic but unambiguous sites of nerve obstruction interspersed within endoneurial tubes with stretches that were clear of debris. We think the difference is explained by the way that electron microscopy study was done: images of nerve cross-section were used. It is possible that the limited coverage of the extent of an axon in cross-section images explains the absence of evidence of endoneurial obstructions in that study.

Although axons inevitably branch to occupy all the primary synaptic folds or gutters at a neuromuscular junction, electron microscopy analysis has long made clear that only one branch typically occupies each primary fold. The reason for the single occupation of folds is unclear, especially given the fact that axons have to branch to occupy all the folds. Our results provide an explanation. By time-lapse imaging of the reinnervation process, we observed many examples of more than one branch within the same fold. However, these cooccupations were always transitory because, when an axon grew into a fold that was also occupied by another branch of the same axon, it underwent growth cone collapse after contacting its sibling branch. The purpose of such avoidance of multiple branches in the same primary gutter is not known, but it may be more efficient for a neuron to support one larger caliber axon branch than multiple small branches within the same region. Interestingly, we show that two or more axon branches from different neurons can more stably cooccupy the same primary folds; a similar result has been seen during early development (Tapia et al., 2012). For this reason, the mechanism for branch removal when the two branches are from the same neurons may best be construed as self-avoidance. This mechanism perhaps may be used in development and reinnervation to discourage two branches of the same axons projecting to the same neuromuscular junction. The self-avoidance may be due to molecular recognition that allows a motor axon to be repulsed by its own surface molecules but not by those of other axons. There is evidence of several different classes of molecules that can mediate self-avoidance (Zipursky and Sanes, 2010; Lefebvre et al., 2012). Further studies to determine which (in any of these) play a role at the neuromuscular junction are under way.

In summary, motor axon regeneration after nerve injury can be divided into two stages: axon regrowth through former endoneurial tubes and reinnervation of vacated AChR sites. The work presented here shows that the slower recovery after denervation in aged animals is largely explained by the slow clearance of nerve and myelin debris from endoneurial tubes by Schwann cells and/or macrophages. The remnants of former nerves act as a barrier that impedes nerve growth. Once axons get past these barriers, they quickly reoccupy former AChR sites, even in very old animals. This reoccupation requires that they branch extensively at the neuromuscular junction site, but they do so without sending multiple branches to the same region by virtue of a powerful axonal self-avoidance mechanism that is active in both young and old animals.

Notes

Supplemental material for this article is available at http://cbs.fas.harvard.edu/Lichtman-Kang-JNeurosci. Movie 1 corresponds to Figure 1*C*; Movie 2 to Figure 3*A–C*; Movie 3 to Figure 4*A*; Movie 4 to Figure 5*A*; and Movie 5 to Figure 5*B*. This material has not been peer reviewed.

References

Black MM, Lasek RJ (1979) Slowing of the rate of axonal regeneration during growth and maturation. Exp Neurol 63:108–119. CrossRef Medline

Bosse F (2012) Extrinsic cellular and molecular mediators of peripheral axonal regeneration. Cell Tissue Res 349:5–14. CrossRef Medline

Brunetti M, Miscena A, Salviati A, Gaiti A (1987) Effect of aging on the rate of axonal transport of choline-phosphoglycerides. Neurochem Res 12: 61–65. CrossRef Medline

Feng G, Mellor RH, Bernstein M, Keller-Peck C, Nguyen QT, Wallace M, Nerbonne JM, Lichtman JW, Sanes JR (2000) Imaging neuronal subsets in transgenic mice expressing multiple spectral variants of GFP. Neuron 28:41–51. CrossRef Medline

Ferguson TA, Son YJ (2011) Extrinsic and intrinsic determinants of nerve regeneration. J Tissue Eng 2:2041731411418392. CrossRef Medline

Filbin MT (2003) Myelin-associated inhibitors of axonal regeneration in the adult mammalian CNS. Nat Rev Neurosci 4:703–713. CrossRef Medline

Kang H, Tian L, Son YJ, Zuo Y, Procaccino D, Love F, Hayworth C, Trachtenberg J, Mikesh M, Sutton L, Ponomareva O, Mignone J, Enikolopov G, Rimer M, Thompson W (2007) Regulation of the intermediate filament protein nestin at rodent neuromuscular junctions by innervation and activity. J Neurosci 27:5948–5957. CrossRef Medline

Kawabuchi M, Chongjian Z, Islam AT, Hirata K, Nada O (1998) The effect of aging on the morphological nerve changes during muscle reinnervation after nerve crush. Restor Neurol Neurosci 13:117–127. Medline

Kawabuchi M, Tan H, Wang S (2011) Age affects reciprocal cellular interactions in neuromuscular synapses following peripheral nerve injury. Ageing Res Rev 10:43–53. CrossRef Medline

Kerschensteiner M, Reuter MS, Lichtman JW, Misgeld T (2008) Ex vivo

imaging of motor axon dynamics in murine triangularis sterni explants. Nat Protoc 3:1645–1653. CrossRef Medline

Komiyama A, Suzuki K (1992) Age-related differences in proliferative responses of Schwann cells during Wallerian degeneration. Brain Res 573: 267–275. CrossRef Medline

Lefebvre JL, Kostadinov D, Chen WV, Maniatis T, Sanes JR (2012) Protocadherins mediate dendritic self-avoidance in the mammalian nervous system. Nature 488:517–521. CrossRef Medline

Livet J, Weissman TA, Kang H, Draft RW, Lu J, Bennis RA, Sanes JR, Lichtman JW (2007) Transgenic strategies for combinatorial expression of fluorescent proteins in the nervous system. Nature 450:56–62. CrossRef Medline

Martini R (1994) Expression and functional roles of neural cell surface molecules and extracellular matrix components during development and regeneration of peripheral nerves. J Neurocytol 23:1–28. CrossRef Medline

McKerracher L, David S, Jackson DL, Kottis V, Dunn RJ, Braun PE (1994) Identification of myelin-associated glycoprotein as a major myelin-derived inhibitor of neurite growth. Neuron 13:805–811. CrossRef Medline

McQuarrie IG, Lasek RJ (1989) Transport of cytoskeletal elements from parent axons into regenerating daughter axons. J Neurosci 9:436–446. Medline

Misgeld T, Kerschensteiner M, Bareyre FM, Burgess RW, Lichtman JW (2007) Imaging axonal transport of mitochondria in vivo. Nat Methods 4:559–561. CrossRef Medline

Mukhopadhyay G, Doherty P, Walsh FS, Crocker PR, Filbin MT (1994) A novel role for myelin-associated glycoprotein as an inhibitor of axonal regeneration. Neuron 13:757–767. CrossRef Medline

Nguyen QT, Sanes JR, Lichtman JW (2002) Pre-existing pathways promote precise projection patterns. Nat Neurosci 5:861–867. CrossRef Medline

Pestronk A, Drachman DB, Griffin JW (1980) Effects of aging on nerve sprouting and regeneration. Exp Neurol 70:65–82. CrossRef Medline

Rich MM, Lichtman JW (1989) In vivo visualization of pre- and postsynaptic changes during synapse elimination in reinnervated mouse muscle. J Neurosci 9:1781–1805. Medline

Sanderson MJ, Parker I (2003) Video-rate confocal microscopy. Methods Enzymol 360:447–481. CrossRef Medline

Schäfer M, Fruttiger M, Montag D, Schachner M, Martini R (1996) Disruption of the gene for the myelin-associated glycoprotein improves axonal regrowth along myelin in C57BL/Wlds mice. Neuron 16:1107–1113. CrossRef Medline

Tanaka K, Webster HD (1991) Myelinated fiber regeneration after crush injury is retarded in sciatic nerves of aging mice. J Comp Neurol 308:180–187. CrossRef Medline

Tapia JC, Wylie JD, Kasthuri N, Hayworth KJ, Schalek R, Berger DR, Guatimosim C, Seung HS, Lichtman JW (2012) Pervasive synaptic branch removal in the mammalian neuromuscular system at birth. Neuron 74: 816–829. CrossRef Medline

Tashiro T, Komiya Y (1994) Impairment of cytoskeletal protein transport due to aging or beta,beta'-iminodipropionitrile intoxication in the rat sciatic nerve. Gerontology 40(suppl 2):36–45. Medline

Uchida Y, Tomonaga M (1987) Loss of nerve growth factor receptors in sympathetic ganglia from aged mice. Biochem Biophys Res Comm 146: 797–801. CrossRef Medline

Valdez G, Tapia JC, Kang H, Clemenson GD Jr, Gage FH, Lichtman JW, Sanes JR (2010) Attenuation of age-related changes in mouse neuromuscular synapses by caloric restriction and exercise. Proc Natl Acad Sci U S A 107:14863–14868. CrossRef Medline

Vaughan DW (1992) Effects of advancing age on peripheral nerve regeneration. J Comp Neurol 323:219–237. CrossRef Medline

Verdú E, Butí M, Navarro X (1995) The effect of aging on efferent nerve fibers regeneration in mice. Brain Res 696:76–82. CrossRef Medline

Verdú E, Ceballos D, Vilches JJ, Navarro X (2000) Influence of aging on peripheral nerve function and regeneration. J Peripher Nerv Syst 5:191–208. CrossRef Medline

Young JZ (1974) Functional recovery after lesions of the nervous system. VI. Conclusion: functional recovery in vertebrates and invertebrates. Neurosci Res Program Bull 12:273–275. Medline

Zipursky SL, Sanes JR (2010) Chemoaffinity revisited: dscams, protocadherins, and neural circuit assembly. Cell 143:343–353. CrossRef Medline

Zuo Y, Lubischer JL, Kang H, Tian L, Mikesh M, Marks A, Scofield VL, Maika S, Newman C, Krieg P, Thompson WJ (2004) Fluorescent proteins expressed in mouse transgenic lines mark subsets of glia, neurons, macrophages, and dendritic cells for vital examination. J Neurosci 24:10999–11009. CrossRef Medline